

Original Research

# Disulfiram/Copper Induce Ferroptosis in Triple-Negative Breast Cancer Cell Line MDA-MB-231

Meiran Chu<sup>1,2,†</sup>, Xinglan An<sup>1,†</sup>, Cong Fu<sup>1</sup>, Hao Yu<sup>3</sup>, Daoyu Zhang<sup>1</sup>, Qi Li<sup>1</sup>, Xi Xia Man<sup>1</sup>, Xiangpeng Dai<sup>1</sup>, Ziyi Li<sup>1,\*</sup> <sup>1</sup>Key Laboratory of Organ Regeneration and Transplantation of Ministry of Education, First Hospital, Jilin University, 130021 Changchun, Jilin, China<sup>2</sup>College of Veterinary Medicine, Jilin University, 130062 Changchun, Jilin, China<sup>3</sup>College of Animal Science, Jilin University, 130062 Changchun, Jilin, China\*Correspondence: [ziyi@jlu.edu.cn](mailto:ziyi@jlu.edu.cn) (Ziyi Li)

†These authors contributed equally.

Academic Editor: Alfonso Urbanucci

Submitted: 29 August 2022 Revised: 20 December 2022 Accepted: 3 January 2023 Published: 28 August 2023

## Abstract

**Background:** The complex formed by disulfiram (DSF) and copper (Cu) is safe and effective for the prevention and treatment of triple-negative breast cancer (TNBC). Although previous studies have shown that DSF/Cu induces ferroptosis, the mechanism remains unclear. **Methods:** The mitochondrial morphology of TNBC treated with DSF/Cu was observed by transmission microscopy, and intracellular levels of iron, lipid reactive oxygen species (ROS), malondialdehyde, and glutathione were evaluated to detect the presence of ferroptosis. Target genes for the DSF/Cu-activated ferroptosis signaling pathway were examined by transcriptome sequencing analysis. Expression of the target gene, *HMOX1*, was detected by qRT-PCR, immunofluorescence and western blot. **Results:** The mitochondria of TNBC cells were significantly atrophied following treatment with DSF/Cu for 24 h. Addition of DSF/Cu supplement resulted in significant up-regulation of intracellular iron, lipid ROS and malondialdehyde levels, and significant down-regulation of glutathione levels, all of which are important markers of ferroptosis. Transcriptome analysis confirmed that DSF/Cu activated the ferroptosis signaling pathway and up-regulated several ferroptosis target genes associated with redox regulation, especially heme oxygenase-1 (HMOX-1). Inhibition of ferroptosis by addition of the ROS scavenger N-acetyl-L-cysteine (NAC) significantly increased the viability of DSF/Cu-treated TNBC cells. **Conclusions:** These results show that DSF/Cu increases lipid peroxidation and causes a sharp increase in HMOX1 activity, thereby inducing TNBC cell death through ferroptosis. DSF/Cu is a promising therapeutic drug for TNBC and could lead to ferroptosis-mediated therapeutic strategies for human cancer.

**Keywords:** DSF/Cu; TNBC; ferroptosis; HMOX1

## 1. Introduction

The cell death process is of fundamental importance for normal human growth, development, disease, and the maintenance of tissue homeostasis [1]. It can be divided into accidental cell death and programmed cell death. Programmed cell death is regulated by specific and intrinsic cellular mechanisms [2]. Traditionally, apoptosis was considered to be the major regulated and programmed pathway of cell death [3]. The induction of cell apoptosis has been investigated as the mainstay of regulated cell death in cancer treatment strategies. More recently, additional modes of programmed cell death have come to light, including autophagy, necrosis, pyroptosis and ferroptosis [4]. There is growing recognition that activation of other regulated cell death mechanisms may be beneficial for cancer treatment, for example in overcoming drug resistance and in providing new drug targets [5].

Ferroptosis is a non-apoptotic type of regulated cell death that differs from general autophagy, apoptosis and necrosis at biochemical, morphological, and genetic levels [6]. It occurs as a result of the iron-dependent, intracel-

lular accumulation of reactive oxygen species (ROS) [7]. Morphologically, ferroptosis is mainly characterized by the shrinkage of mitochondria with condensed and ruptured outer membrane, reduced or absent mitochondrial ridge, and reduced or absent mitochondrial crista [6]. Biochemically, excessive iron can lead to increased accumulation of lipid peroxidation in a Fenton-like reaction, and the depletion of antioxidant glutathione (GSH) that also causes accumulation of lipid ROS [8]. Although ROS play crucial roles in normal cellular and organismal function [9], high ROS levels cause cell injury and death. Increasing evidence suggests that the efficacy of tumor growth suppression can be significantly improved by inducing ferroptosis [10]. Compared to normal cells, cancer cells have an increased iron demand which makes them more vulnerable to iron-catalyzed ferroptosis [11]. Recently, several classic therapeutic drugs (e.g., sulfasalazine, sorafenib, cisplatin, acetaminophen) were confirmed to induce ferroptosis in cancer cells [8]. Targeting ferroptosis might therefore be a new therapeutic approach to cancer treatment.



Numerous studies have identified the disulfiram (DSF)/copper (Cu) complex as a promising anticancer agent against triple-negative breast cancer (TNBC) and other cancers [12]. DSF/Cu was also recently shown to induce ferroptosis in various cancer types [13,14]. Its toxicity is dependent on oxidative stress mechanisms, including the production of peroxide, lipid peroxidation, and mitochondrial damage [15]. Because the changes in oxidative stress in these cells are inextricably linked to ferroptosis, we speculate that DSF/Cu induces ferroptosis in TNBC cells.

DSF/Cu is thought to affect a variety of molecular targets and signaling pathways. In the present study, we investigated the ferroptosis pathway as a possible mechanism by which DSF/Cu inhibits TNBC. To further clarify the regulatory mechanism of ferroptosis induction, we focused on several potential candidate genes including *HMOX1*, *TFRC*, *GPX4*, *ACSL4* and *LPCAT3* [16,17]. The aim of this study was to explore the mechanism underlying the potential antitumor effects of DSF/Cu in the treatment of TNBC.

## 2. Materials and Methods

### 2.1 Reagents

Disulfiram (DSF) was purchased from Selleck (Cat. No: S1680, Houston, TX, USA) and  $\text{CuCl}_2$  from Sigma-Aldrich (Cat. No: 7447-39-4, St. Louis, MO, USA). They were dissolved in dimethyl sulfoxide (DMSO) at a concentration of 50 mM and stored at  $-80^\circ\text{C}$  prior to use. CCK-8 solution was purchased from US Everbright® Inc (Cat. No: C6005M, Silicon Valley, CA, USA). TRIzol reagent was purchased from Invitrogen (Cat. No: 15596026, Carlsbad, CA, USA). SYBR® Premix Ex Taq™ reagents were purchased from TaKaRa (Cat. No: DRR041A, Tokyo, Japan). The Light Cycle® 96 Real-Time PCR System was purchased from Roche (Basel, Switzerland). HMOX1 antibody was purchased from Abcam (Cat. No: ab13243, Cambridge, UK) and GAPDH antibodies from Proteintech (Cat. No: 60004-1-Ig, Wuhan, Hubei, China). The Glutathione Assay Kit and Lipid Peroxidation MDA Assay Kit were purchased from Beyotime (Cat. No: S0058, S0131M, Shanghai, China). The JC-1 MitoMP Detection Kit (Cat. No: MT09) and FerroOrange were purchased from Dojindo Molecular Technologies Company (Cat. No: F374, Kumamoto, Kyushu, Japan).

### 2.2 Cell Culture

DSF and Cu were freshly mixed at a ratio of 1:1.7 prior to use. The human TNBC cell line MDA-MB-231 (Cat. No. CL-0150B) was purchased from Procell Life Science & Technology Co., Ltd. (Wuhan, Hubei, China). MDA-MB-231 was grown in RPMI 1640 medium (Cat. No: R8758-500ML, Gibco, Big Island, NY, USA) supplemented with 10% fetal bovine serum (FBS, Cat. No: F8687) and 1% penicillin-streptomycin solution (Cat. No: SV30010, Gibco, Big Island, NY, USA). All cells were cultured at  $37^\circ\text{C}$  in a 5%  $\text{CO}_2$  atmosphere. The cell lines were

authenticated using Short Tandem Repeat (STR) profiling within the last three years. All experiments were performed with mycoplasma-free cells.

### 2.3 Transmission Electron Microscopy (TEM)

MDA-MB-231 cells were seeded into 6-well plates at  $2 \times 10^5$  cells per well. After 24 h, cells were treated with DSF/Cu (0.2  $\mu\text{M}$ /0.2  $\mu\text{M}$ ) and incubated for 12 or 24 h. Cells were then harvested and fixed in a droplet of 2% glutaraldehyde overnight at  $4^\circ\text{C}$ . Samples were processed and observed by TEM (HT7700, HITACHI, Tokyo, Japan).

### 2.4 Detection of Mitochondrial Membrane Potential

Cells were assessed for mitochondrial function using a fluorescent JC-1 probe according to the manufacturer's protocol [18]. JC-1 accumulates in healthy mitochondria and is red fluorescent. At the collapse of mitochondrial potential, the red/green fluorescent intensity ratio reflects membrane depolarization. TNBC cells ( $2.5 \times 10^5$  cells per well) were seeded into 6-well plates and incubated with culture medium. The next day, cells were treated with 0.1% DMSO or DSF/Cu and incubated for 24 h. The medium was then removed and 10  $\mu\text{g}/\text{mL}$  JC-1 was added for a 10-minute incubation. After washing thrice, the cells were examined using a fluorescent microscope (Ti2-U, Nikon, Tokyo, Japan) equipped with a digital camera. All pictures were taken using the same microscope settings and exposure times.

### 2.5 RNA Sequencing

To determine the transcriptome changes caused by DSF/Cu, RNA was extracted by TRIzol reagent from MDA-MB-231 cells following 24 h treatment with DSF/Cu. The construction and RNA-Seq analysis were carried out by Lianchuan Company (Hangzhou, Zhejiang, China).

### 2.6 RNA Isolation and qPCR Analysis

Total RNA was extracted from MDA-MB-231 TNBC cells using TRIzol reagent according to the manufacturer's instructions. A total of 500 ng of RNA per sample was reverse-transcribed into cDNA with TransScript All-in-One-First-Strand cDNA Synthesis Super Mix for qPCR (Cat. No: AT321-01, TRAN, TRAN, Shanghai, China). Briefly, qPCR was performed using FastStart Essential DNA Green Master (Cat. No: 4913914001, Roche, Basel, USA). The  $2^{-\Delta\Delta\text{Ct}}$  method was used to calculate the average relative fold-change in mRNA expression. Primers sequences are shown in **Supplementary Table 1**.

### 2.7 Survival Analysis

The gene expression profiles (RNA-seq) and related clinical information of 1226 breast cancer patients were downloaded from UCSC Xena (<http://xena.ucsc.edu/>) [19]. 110 TNBC patients (*breast carcinoma estrogen receptor status* = 'Negative', *breast carcinoma progesterone recep-*

*tor status = 'Negative', lab proc her2 neu immunohistochemistry receptor status = 'Negative')* were selected for further analysis. The transcription expression value from RNA seq was shown as  $\log_2(x + 1)$  transformed RSEM normalized count. The expression level of each selected genes in each sample was defined as high or low by using “survminer” package (Release 0.4.9) [20] in R software (version 4.2.1) [21]. And then, survival analysis was conducted using the Kaplan–Meier plot and Cox’s proportional hazard regression (HR) model, R package “survival” (Release 3.4-0) [22] was used to accomplish this part. HR (95% CI) and p value of each gene was modified based on profile penalized maximum likelihood bias reduction method by using R package “coxphf” (Release 1.13.1, <https://CRAN.R-project.org/package=coxphf>). The results were considered statistically significant if Log rank *p* value was less than 0.05.

## 2.8 Western Blot Analysis

Cells were collected by 0.25% trypsinization, washed in ice-cold phosphate buffer saline (PBS) and then lysed in radio immunoprecipitation assay lysis (RIPA) buffer. The protein concentration was quantified using a BCA Protein Assay Kit purchased from Thermo Fisher Scientific (Cat. No. 23227, Waltham, MA, USA). Western blot analysis was conducted using the antibodies described above and the immunoblotting method described in our previous study [23]. Briefly, equal amounts of protein were subjected to SDS-PAGE and transferred to polyvinylidene difluoride membranes purchased from Merck Millipore (Cat. No: IPVH15150, Darmstadt, Germany). The membranes were blocked with 5% BSA or fat-free milk and incubated at 4 °C overnight with primary antibodies (1:1000 dilution) before washing three times in TBS-T. The membranes were then incubated with secondary antibody (1:2000) at room temperature for 1 h and washed three times in TBS-T. Immunoreactive protein bands were visualized using High-sig ECL Western Blotting Substrate (Cat. No: 180-5001, Tanon, Shanghai, China).

## 2.9 Immunofluorescence Analysis

The method described in our previous study [23]. Cells were grown on cover slides in a 24-well plate and then treated with DSF/Cu (0.2  $\mu$ M/0.34  $\mu$ M) for 48 h. After treatment, cells were fixed with 4% paraformaldehyde for 30 min and then permeabilized with 0.1% Triton X-100 for 15 min. The cells were blocked with 2% bovine serum albumin (BSA) for 1 h and then incubated overnight at 4 °C with primary antibodies. After washing thrice, the cells were incubated with a Goat Anti-Rabbit/Mouse IgG (Proteintech, Wuhan, Hubei, China) secondary antibody in the dark for 1.5 h and then stained with 0.5  $\mu$ g/mL 4,6-diamino-2-phenyl indole (DAPI) for 15 min. The samples were examined using a fluorescent microscope (Ti2-U, Nikon,

Tokyo, Japan) equipped with a digital camera. All pictures were taken using the same microscope settings and exposure times.

## 2.10 Detection of Mitochondrial Labile Iron

The MDA-MB-231 cells were treated with DSF/Cu for 6, 12 or 24 h. The culture medium was then removed and the cells washed three times with PBS. FerroOrange working solution diluted in serum-free medium to a concentration of 1  $\mu$ M was added and incubated at 37 °C in a 5% CO<sub>2</sub> incubator for 30 min. The samples were examined using a fluorescent microscope (Ti2-U, Nikon, Tokyo, Japan) equipped with a digital camera. All images were taken using the same microscope settings and exposure times.

## 2.11 Glutathione (GSH) Measurement

Cellular GSH levels were measured using the Glutathione Assay Kit (S0053, Beyotime, Shanghai, China) as recommended by the manufacturer. Briefly, MDA-MB-231 cells were seeded into 6-well plates at  $2 \times 10^5$  cells per well. The next day, cells were treated with DMSO or DSF/Cu and incubated for 24 h. Cells were then washed with PBS and collected into a 1.5 mL EP tube. Cell pellets (10  $\mu$ L) were mixed with 30  $\mu$ L of the protein removal reagent M solution. The samples were then frozen and thawed twice using liquid nitrogen and 37 °C water. They were centrifuged at 10,000 g for 10 min and the supernatant used for GSH measurement with a Varioskan Flash Multimode Reader (Varioskan LUX, Thermo Scientific, Waltham, MA, USA) at 412 nm. All assays were performed in triplicate.

## 2.12 Malondialdehyde (MDA) Level Measurement

The cells MDA concentration was assessed using Lipid Peroxidation MDA Assay Kit (Cat.No.S0131S, Beyotime, Shanghai, China). In brief, MDA-MB-231 cells were seeded in a 6-well cell plates at  $2 \times 10^5$  cells. The next day, cells were treated with DMSO or DSF/Cu and incubated for 24 h. Cells were washed with PBS, then collected into a 1.5 mL EP tube and lysed in RIPA buffer. The lysed cells were centrifuged at 10,000 g for 10 min and the supernatant was collected. Then, the supernatant was incubated with an equal volume of thiobarbituric acid buffer (TAB) at 100 °C for 15 minutes. The MDA levels were measured by a Varioskan Flash Multimode Reader (Varioskan LUX, Thermo Scientific, Waltham, MA, USA) at 532 nm. All assays were replicated in triplicate.

## 2.13 Statistical Analysis

All experimental data are expressed as the mean value  $\pm$  standard deviation (SD). qPCR data were analyzed with Prism 7 (GraphPad, LA Jolla, CA, USA) by Student’s *t*-test and one-way ANOVA. *p* < 0.05 was considered statistically significant. For the gene integration analysis, a false discovery rate (FDR)-adjusted *p*-value of  $\leq 0.05$  and

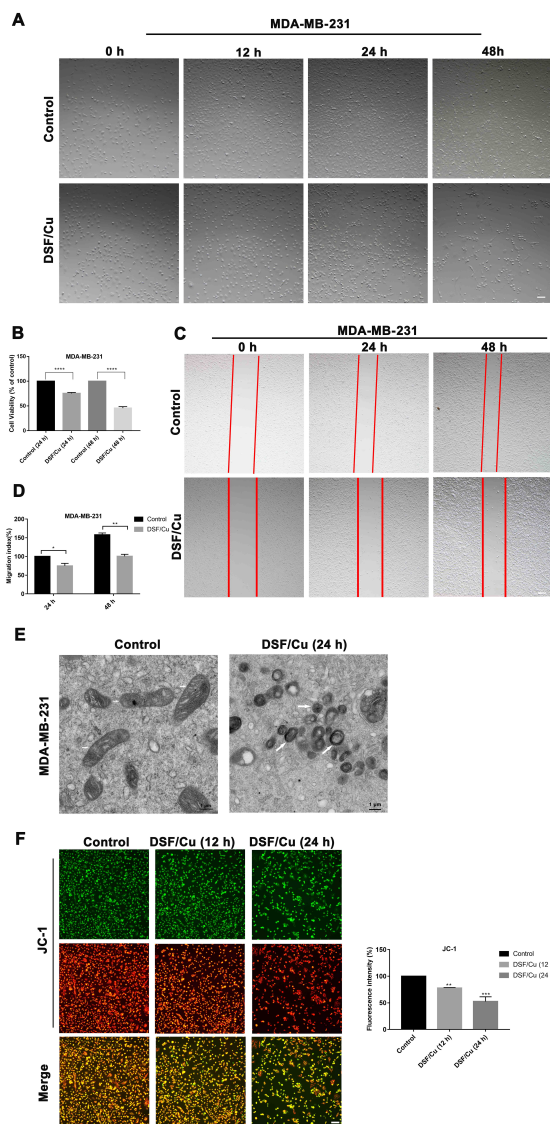


**Fig. 1. DSF/Cu impaired the mitochondria in TNBC cells.** (A) DSF/Cu impairs the mitochondria in TNBC cells. The cellular morphology of MDA-MB-231 cells following treatment with DMSO or DSF/Cu (0.2  $\mu$ M/0.34  $\mu$ M) for 12 h, 24 h or 48 h. Scale bar: 10  $\mu$ m. (B) Relative cell viability in MDA-MB-231 cells was measured by CCK-8 assay (mean  $\pm$  SD, n = 3) after 48 h treatment with 6-TG or/and DSF/Cu. (C,D) Wound healing assays were used to examine the cell migration in MDA-MB-231 cells following exposure to DSF/Cu (0.2  $\mu$ M/0.34  $\mu$ M) for 24 h, 48 h. Scale bar: 10  $\mu$ m. (E) Transmission electron microscopy images of MDA-MB-231 cells after treatment with DSF/Cu for 24 h. Arrows indicate the mitochondria in cells. Scale bar: 1  $\mu$ m. (F) Representative fluorescence images of JC-1 staining in MDA-MB-231 cells treated with DSF/Cu (0.2  $\mu$ M/0.34  $\mu$ M) for 12 h and 24 h. The data are presented as the mean  $\pm$  SD of three replicates. \*p value < 0.1, \*\*p value < 0.01, \*\*\*p value < 0.001 and \*\*\*\*p value < 0.0001 compared to controls.

an absolute value of log<sub>2</sub> fold-change (FC)  $\geq 2$  was used as thresholds to define significant differences in gene expression.

### 3. Results

#### 3.1 DSF/Cu Impairs Mitochondria in TNBC Cells

To examine the inhibitory effect of DSF/Cu on TNBC cells, MDA-MB-231 cells were treated with 0.2  $\mu$ M DSF and 0.34  $\mu$ M CuCl<sub>2</sub> for various times. The optimal concentration of DSF/Cu was determined in our previous study [23]. The effect of DSF/Cu on the morphology of TNBC cells was investigated using an inverted microscope (Fig. 1A). Compared to the control group, MDA-MB-231 cells treated with DSF/Cu for 6 h, 12 h, 24 h and 48 h showed varying degrees of shrinkage, roundness, and multidirectional. We measured cell survival by CCK-8 assay. Six thousand cells per well were plated and cultured in a 96-well dish for 24 h. Then, the cells were treated with different concentrations of 6-TG and DSF/Cu for 48 h. Compared with that of the control cell lines, the proliferation of the cell lines treated with the DSF/Cu was significantly inhibited. (Fig. 1B). Furthermore, we used wound healing assays to examine the effect of DSF/Cu on MDA-MB-231 cells. The metastatic capacity of cells treated with DSF/Cu was significantly lower than that of cells treated with DMSO (Fig. 1C,D).

To further examine the effect of DSF/Cu on the ultrastructure of TNBC cells, MDA-MB-231 cells were treated for 12 h and 24 h and then observed by TEM. Treated cells did not show the characteristic morphological hallmarks of apoptosis. The mitochondria of TNBC cells became smaller and showed increased membrane density, while the mitochondrial cristae decreased in size or disappeared, suggesting that DSF/Cu may cause ferroptosis in these cells (Fig. 1E). To further examine the effect of DSF/Cu on mitochondrial function, JC-1 staining was used to visualize the mitochondrial membrane potential (MMP). JC-1 accumulates in healthy mitochondria and exhibits red fluorescence. When the mitochondrial potential collapses, the fluorescence changes from red to green. The red fluorescence JC-1 polymer and green fluorescence JC-1 monomer were photographed by fluorescence microscope. ImageJ software (version: V1.8.0.112, LOCI, University of Wisconsin, Madison, WI, USA) for mixed channels. MMP was evaluated by the fluorescence intensity ratio of red to green. Immunofluorescence analysis showed that DSF/Cu decreased the MMP in MDA-MB-231 cells compared to control cells (Fig. 1F).

#### 3.2 DSF/Cu-Induced Cytotoxicity in TNBC Cells is Mediated by ROS

Lipid peroxidation driven by oxidative stress is an important cytotoxic factor in ferroptosis. We therefore used the fluorochrome Liperfluor to examine the effect of DSF/Cu on lipid peroxidation levels in MDA-MB-231

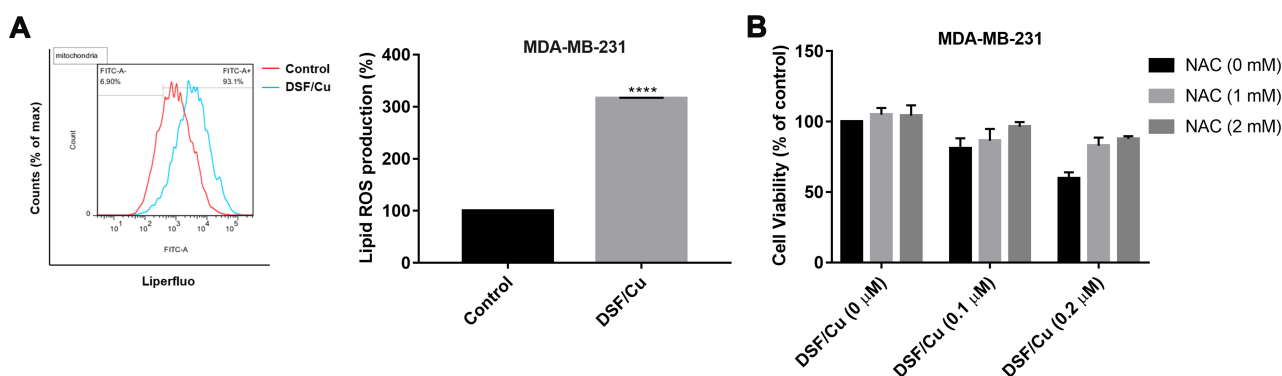


**Fig. 2. DSF/Cu-induced cytotoxicity in TNBC cells is mediated by ROS.** (A) Cellular lipid ROS detected by the Liperfluo fluorescent probe. DSF/Cu treatment increased the lipid peroxidation level. (B) MDA-MB-231 cells pretreated with 1- or 2-mM NAC were co-incubated with DSF/Cu (0.1/0.17 or 0.2/0.34  $\mu$ M) for 24 h and their viability then tested using the CCK8 kit. Results are presented as the mean  $\pm$  SD of three replicates. \*\*\*\* $p$  value  $<$  0.0001 compared to controls.

cells. Treatment with DSF/Cu for 24 h was observed to increase lipid peroxidation in MDA-MB-231 cells, while co-treatment with the ROS scavenger N-acetyl-L-cysteine (NAC) reversed this increase (Fig. 2A). Furthermore, we also found that ROS scavenger NAC could partially reverse the death of MDA-MB-231 cells induced by DSF/Cu (Fig. 2B). Furthermore, NAC partially prevented the death of MDA-MB-231 cells induced by DSF/Cu (Fig. 2B). These results indicate that DSF/Cu can induce lipid peroxidation and morphological changes in mitochondria.

### 3.3 DSF/Cu Regulation of Ferroptosis Biomarkers

Key biomarkers of ferroptosis are iron accumulation, GSH depletion, and lipid peroxidation [24]. To further investigate whether ferroptosis is implicated in DSF/Cu-induced tumor inhibition, we evaluated the levels of intracellular labile Fe (II), GSH, and the oxidative stress marker malondialdehyde (MDA) in MDA-MB-231 treated with DSF/Cu. The FerroOrange probe was used to examine the intracellular labile Fe (II) content in MDA-MB-231 cells after DSF/Cu treatment for 6, 12 and 24 h. In MDA-MB-231 cells, a time-dependent increase in labile Fe (II) was observed in response to DSF/Cu (Fig. 3A).

We next examined the levels of intracellular GSH and of the oxidative stress marker MDA. Following treatment with DSF/Cu, the GSH level showed a significant 10-fold decrease compared to controls (Fig. 3B), indicating marked GSH depletion. In contrast, the oxidative stress marker MDA showed markedly increased levels in MDA-MB-231 cells following treatment with DSF/Cu (Fig. 3C). We selected ferrostatin-1 (Fer-1), one of the ferroptosis inhibitors, and detected cell viability by CCK-8 to evaluate whether Fer-1 can save DSF/Cu-induced ferroptosis in triple negative breast cancer cells. The results showed that the addition of ferroptosis inhibitor inhibited the death of triple negative breast cancer cells caused by DSF/Cu, indicating that DSF/Cu induced the ferroptosis of triple negative

breast cancer cells (Fig. 3D). Taken together, the above findings on critical ferroptosis biomarkers strongly suggest that DSF/Cu triggers ferroptosis in TNBC cells.

### 3.4 DSF/Cu Regulates Ferroptosis Pathway Gene Expression

To investigate whether DSF/Cu triggers ferroptosis at the transcriptional level, we performed transcriptome sequencing of MDA-MB-231 cells after treatment with DSF/Cu (0.2  $\mu$ M/0.34  $\mu$ M) for 24 h. To reduce the number of false positives, three biological replicates were used to compare the transcriptomes of control and DSF/Cu-treated cells. The significantly differentially expressed genes in RNA Seq were counted by volcano diagram, and the more differentially expressed genes were distributed at both ends. The red dots represent genes whose expression level of control in the sample is up-regulated compared with that of the control sample, and the blue dots represent down-regulated genes, among which 874 genes are up-regulated and 764 genes are down-regulated (Fig. 4A). Subsequently, we selected the most significant up- and down-regulated top 100 gene and established heat maps to cluster the significantly different genes (Fig. 4B). We also performed KEGG analysis to identify significant pathways that had been altered after DSF/Cu treatment, and found that 20 signaling pathways were significantly enriched. The results showed that TNBC cell death induced by DSF/Cu was associated with the MAPK signaling pathway, p53 signaling pathway, mitophagy signaling pathway, and ferroptosis (Fig. 4C).

qRT-PCR was performed to confirm the results of RNA-seq. Consistent with the RNA-seq data, the mRNAs for prostaglandin-endoperoxide synthase 2 (*PTGS2*), cation transport regulator-like protein 1 (*CHAC1*), spermidine/spermine N1-acetyltransferase 1 (*SAT1*), transferrin receptor protein 1 (*TFRC*), heme oxygenase-1 (*HMOX1*) were found to be up-regulated after 12 h and 24 h of DSF/Cu treatment. In contrast, the mRNAs for glutathione perox-

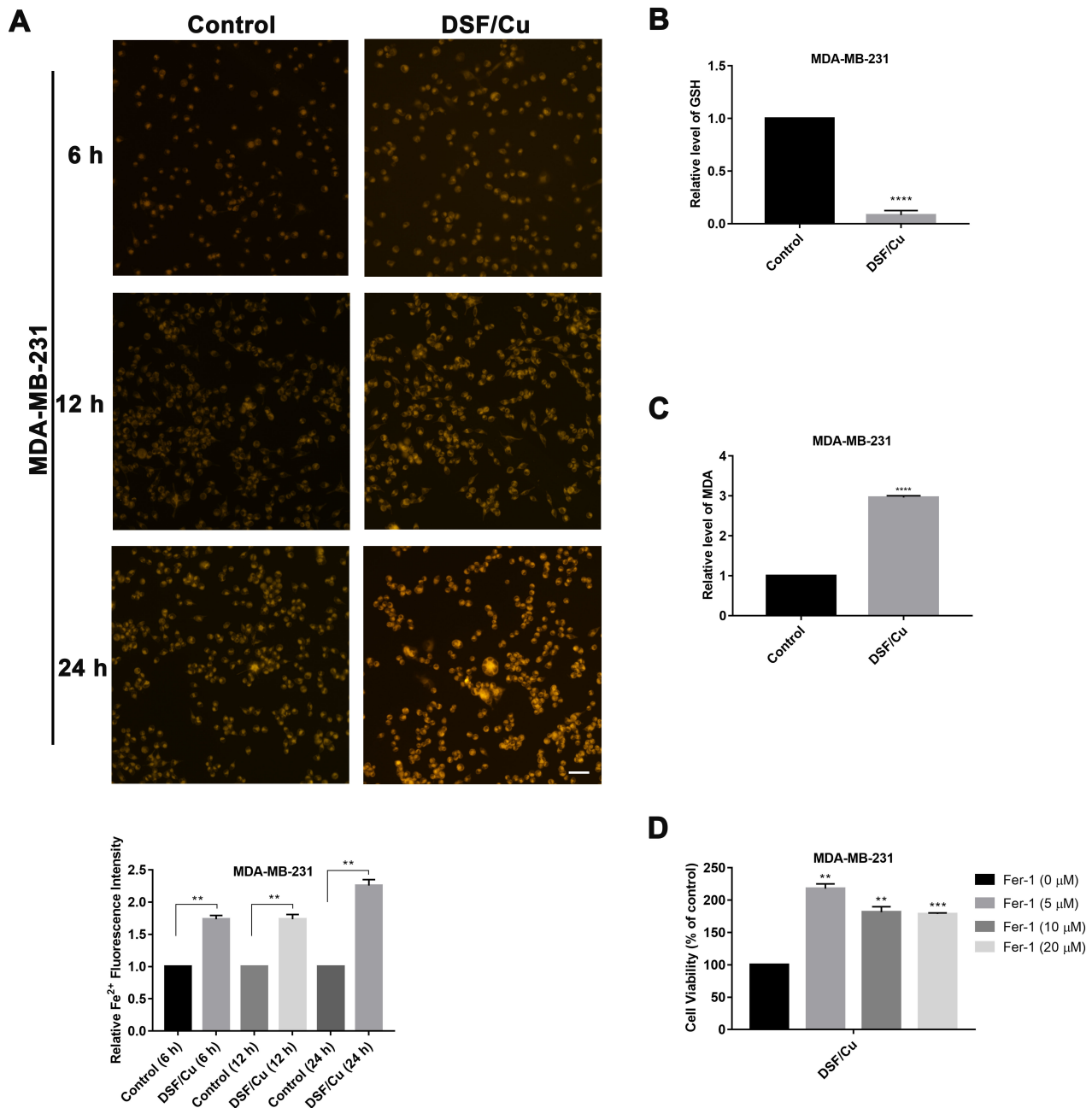


**Fig. 3. DSF/Cu regulates ferroptosis biomarkers.** (A) MDA-MB-231 cells were treated with DSF/Cu (0.2  $\mu\text{M}$ /0.34  $\mu\text{M}$ ) for 6, 12 and 24 h and then collected to visualize the intracellular  $\text{Fe}^{2+}$  ion level using the fluorescent probe FerroOrange. Scale bar: 20  $\mu\text{m}$ . (B) MDA-MB-231 cells were treated with DSF/Cu (0.2  $\mu\text{M}$ /0.34  $\mu\text{M}$ ) for 24 h and the level of glutathione was then measured. (C) MDA-MB-231 cells were treated with DSF/Cu (0.2  $\mu\text{M}$ /0.34  $\mu\text{M}$ ) for 24 h and the level of MDA was then measured. (D) The MDA-MB-231 cells pretreated by 5, 10, 20  $\mu\text{M}$  Fer-1 were co-incubated with (0.2, 0.34)  $\mu\text{M}$  DSF/Cu for 24 h, and the cell viability was tested by CCK8 kit. The data are presented as the mean  $\pm$  SD of three replicates. \*\* $p$  value < 0.01, \*\*\* $p$  value < 0.001 and \*\*\*\* $p$  value < 0.0001 compared to controls.

idase 4 (*GPX4*), ferroportin (*SLC40A1*) and Fanconi anemia complementation group D2 (*FANCD2*) were down-regulated after 12 h and 24 h of treatment (Fig. 4D). *GPX4* is an antioxidant enzyme thought to be an essential suppressor of ferroptosis by using GSH as the substrate. The expression of *GPX4* in DSF/Cu-treated cells decreased sig-

nificantly after treatment with DSF/Cu, consistent with the observed depletion of GSH. The results of qRT-PCR suggested that among the genes involved in the ferroptosis pathway, the *HMOX1* gene is the most significantly up-regulated gene.

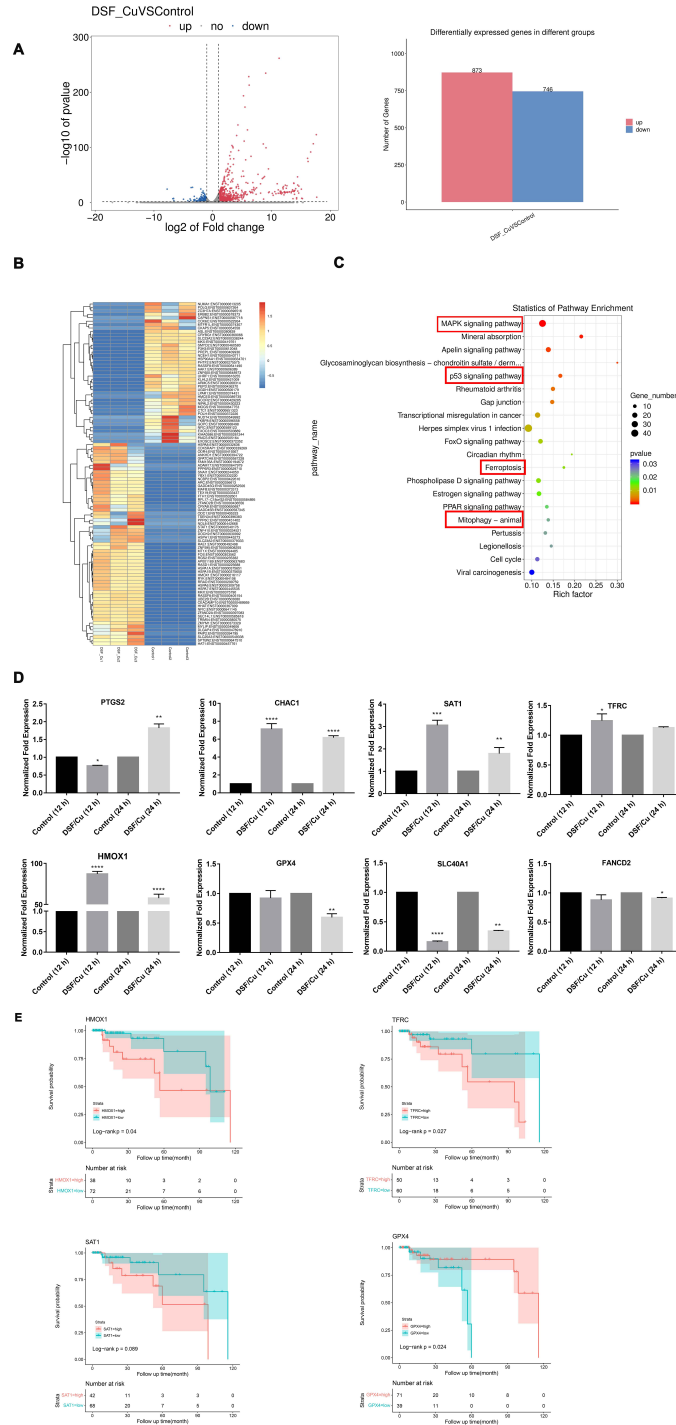


**Fig. 4. DSF/Cu treatment induced transcriptome alteration.** (A) Volcano plot showing the differences in RNA expression by DSF/Cu (0.2  $\mu$ M /0.34  $\mu$ M) treatment, as detected in MDA-MB-231 cells using RNA Seq. The red dots represent genes whose expression level of control in the sample is up-regulated compared with that of the control sample, and the blue dots represent down-regulated genes. (B) Heat map of up-regulated and down-regulated genes with significant difference in expression after DSF/Cu treatment. (C) KEGG pathway analysis showed the significant pathways that had been altered after DSF/Cu treatment. (D) MDA-MB-231 cells were treated with DSF/Cu (0.2  $\mu$ M /0.34  $\mu$ M) for 12, 24 h. Ferroptosis-correlated gene including *PTGS2*, *CHAC1*, *SAT1*, *TFRC*, *HMOX1* were up-regulated. Ferroptosis-correlated gene including *GPX4*, *SLC40A1*, *FANCD2* were down-regulated. (E) Kaplan-Meier survival curves for TNBC patients. Data are shown as means  $\pm$  SD. \* $p < 0.05$ , \*\* $p < 0.01$ , \*\*\* $p < 0.001$  and \*\*\*\* $p$  value  $< 0.0001$ ,  $n = 3$ .

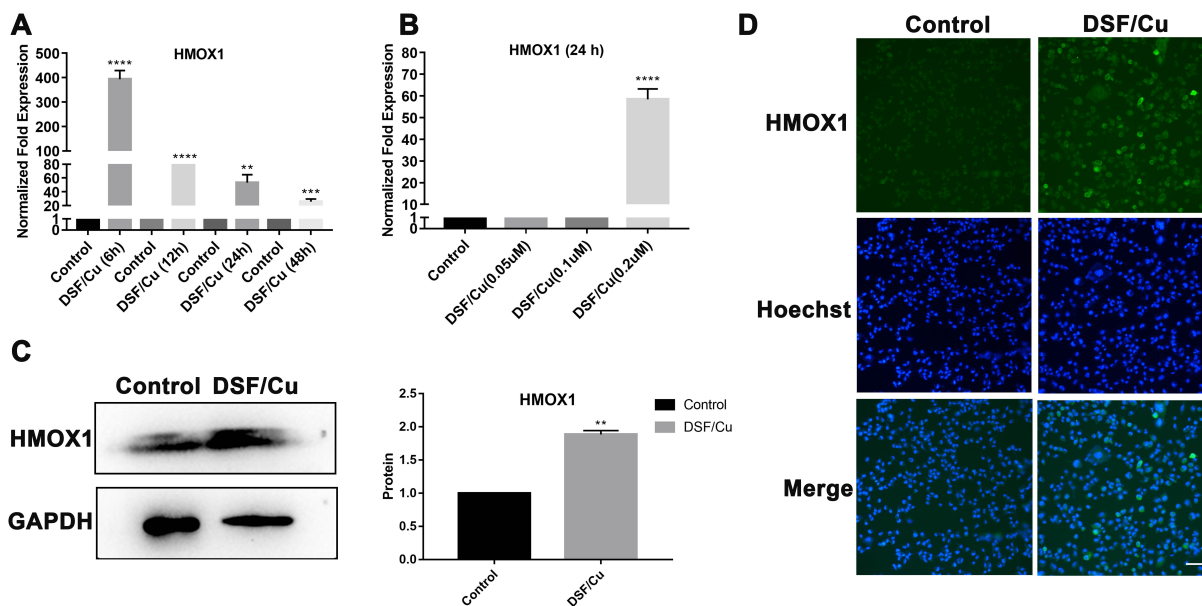


**Fig. 5. DSF/Cu increases cellular HMOX1 expression.** (A) MDA-MB-231 cells were treated with DSF/Cu (0.2  $\mu$ M/0.34  $\mu$ M) for the indicated time intervals (6, 12, 24, 48 h). DSF/Cu-induced *HMOX1* mRNA expression was maximal at 6 h and declined thereafter. (B) MDA-MB-231 cells were incubated with different concentrations of DSF/Cu (0, 0.1, 0.2  $\mu$ M) for 24 h and the expression of *HMOX1* mRNA was analyzed by q-PCR. *GAPDH* was used as a control. The results are presented as the mean  $\pm$  SD of three replicates. (C) Western blot was used to evaluate HMOX1 protein levels in MDA-MB-231 cells treated with DSF/Cu (0.2  $\mu$ M/0.34  $\mu$ M) for 24 h. The results are presented as the mean  $\pm$  SD of three replicates. (D) Immunofluorescence was used to detect HMOX1 expression in MDA-MB-231 cells following exposure to DSF/Cu (0.2  $\mu$ M/0.34  $\mu$ M). Scale bar: 10  $\mu$ m. \*\* $p$  value  $< 0.01$ , \*\*\* $p$  value  $< 0.001$  and \*\*\*\* $p$  value  $< 0.0001$  compared to the controls.

**Table 1. Summary of analysis of genes under Cox's proportional hazards regression model before and after modifying based on profile penalized maximum likelihood bias reduction method.**

Gene	HR	95% CI	p-value
<i>HMOX1</i>	0.327	0.102–0.981	0.046*
<i>TFRC</i>	0.28	0.07–0.889	0.03*
<i>SAT1</i>	0.391	0.122–1.178	0.094
<i>GPX4</i>	3.92	0.141–14.887	0.03*

Abbreviations: CI, confidence interval; HR, hazard ratio; \* $p < 0.05$ .

To investigate the effect of ferroptosis genes in triple negative breast cancer after DSF/Cu treatment, KM survival curve analysis was performed. Survival analysis showed that patients with higher HMOX1 ( $p = 0.046$ , HR = 0.327), TFRC ( $p = 0.03$ , HR = 0.28), SAT1 ( $p = 0.094$ , HR = 0.391) expression and patients with lower GPX4 ( $p = 0.03$ , HR = 3.92) expression had an increased overall survival (Fig. 4E, Table 1).

### 3.5 DSF/Cu Simultaneously Increases Cellular HMOX1 Levels.

The results of transcriptome sequencing suggested that *HMOX1* was the most significantly upregulated gene

amongst those involved in the ferroptosis pathway. One of the major functions of HMOX1 is the release of labile Fe (II) [25]. To further examine this gene in MDA-MB-231 cells treated with DSF/Cu for different times (6, 12, 24, 48 h), we quantified the changes in *HOMX1* mRNA level using qRT-PCR. DSF/Cu-induced *HMOX1* mRNA expression was maximal at 6 h and declined thereafter (Fig. 5A). MDA-MB-231 cells were also treated with different concentrations of DSF/Cu (0.05, 0.1, and 0.2  $\mu$ M) for 24 h. Interestingly, the expression of HMOX1 increased significantly only when the cells were exposed to 0.2  $\mu$ M DSF/Cu (Fig. 5B). The HMOX1 protein level in MDA-MB-231 cells treated with DSF/Cu (0.2  $\mu$ M/0.34  $\mu$ M) for 24 h was also evaluated by Western blot. Consistent with the q-PCR data, DSF/Cu treatment increased the expression of HMOX1 protein (Fig. 5C,D). Immunofluorescence staining for HMOX1 gave a similar result (Fig. 5D). Together, these results suggest that DSF/Cu induces ferroptosis in TNBC cells by increasing the expression of HMOX1.

## 4. Discussion

Ferroptosis has received increased attention recently due to its possible application in cancer therapy, and without the development of drug resistance [26]. The induction of ferroptosis therefore has great potential as a new

approach for anti-tumor therapies. DSF is a highly effective anti-alcoholism drug. In combination with Cu, it has also been investigated for the treatment of various cancer types [27]. Although excellent anticancer efficacy has been shown through its ability to inhibit cancer cell proliferation, the underlying molecular mechanism is far from clear. It is generally believed that DSF/Cu triggers TNBC cell death through apoptosis [28], or by decreasing NF- $\kappa$ B expression and targeting the NPL4 adaptor of p97/VCP [29]. So far, a few studies have reported that DSF/Cu can induce ferroptosis in cancer cells. Li *et al.* [13] showed that DSF/Cu could induce ferroptosis in nasopharyngeal cancer cells, while Yang *et al.* [5] found that DSF induced ferroptosis in glioblastoma cells, and Ren *et al.* [14] showed that DSF/Cu induced ferroptosis in hepatocellular carcinoma cells. In the current study, we showed that DSF/Cu activated the ferroptosis cell death pathway in TNBC cells. DSF/Cu treatment resulted in increased lipid peroxidation and a drastic rise in HMOX1 expression, as well as decreased levels of cellular antioxidant and defense-related molecules such as GPX4 and GSH, thereby causing cancer cell death by inducing ferroptosis.

ROS are known to have an important role in the regulation of a variety of biological processes [30]. Cancer cells have excess ROS in comparison to normal cells, in which a redox balance exists [31]. While the elevation of ROS to highly toxic levels can effectively kill cancer cells, excessive ROS can also induce irreparable DNA damage or programmed cell death (e.g., by ferroptosis) [32]. A large number of anticancer drugs have now been identified that kill cancer cells by enhancing ROS generation [33]. Many studies have reported that DSF/Cu treatment results in the accumulation of intracellular ROS [15]. In the present study we observed that DSF/Cu treatment led to an increased level of lipid peroxidation in MDA-MB-231 cells. This is likely to be an important event that explains why cancer cells treated with DSF/Cu are killed by ferroptosis.

HMOX1 is a rate-limiting enzyme in heme catabolism and detoxifies heme to generate free iron, biliverdin and carbon monoxide (CO) in mammalian cells. Upregulation of *HMOX1* therefore increases free iron in the cell, which can then accumulate in mitochondria and cause lipid peroxidation [23]. In the current study, both transcriptome sequencing and RT-qPCR revealed that DSF/Cu significantly induced *HMOX1* mRNA expression and therefore labile Fe (II) in a time-dependent manner in MDA-MB-231 cells. Interestingly, we also found that GSH levels rapidly fell after DSF/Cu treatment of TNBC cells. In contrast, the level of MDA, which is an important product of membrane lipid peroxidation and is positively correlated with ferroptosis, increased following DSF/Cu treatment. These results provide further evidence that DSF/Cu can activate the ferroptosis cell death pathway in TNBC cells.

## 5. Conclusions

This study found that DSF/Cu treatment of TNBC cells increased lipid peroxidation, caused a sharp increase in HMOX1 activity, and reduced the levels of antioxidant cellular defense-related molecules such as GPX4 and GSH, thereby causing cell death by ferroptosis. These findings demonstrate that DSF/Cu is a promising therapeutic drug for TNBC and may be useful in the development of ferroptosis-mediated therapeutic strategies for human cancer.

This study provides a new treatment plan for the treatment of TNBC, and in our previous related studies, we found that this drug can also coordinate with other tumor suppressors. Furthermore, disulfiram/copper can induce iron death not only in tumors but also in other cytological studies such as stem cells, aging, etc.

## Availability of Data and Materials

The datasets generated for this study can be found in the GEO number: GSE209533. The link of dataset is <https://www.ncbi.nlm.nih.gov/geo/query/acc.cgi?acc=gse209533&token=>.

## Author Contributions

Conceived the project and supervised the experiments—ZL. Collected the data—MC, CF, QL and XM. Contributed data or analytical tools—CF, HY and XD. Performed the analysis—XA, DZ and XD. Wrote the paper—MC and XA. All authors contributed to editorial changes in the manuscript. All authors read and approved the final manuscript.

## Ethics Approval and Consent to Participate

Not applicable.

## Acknowledgment

Not applicable.

## Funding

This work was supported by National Natural Science Foundation of China (No: 31972874), National Key R&D Program of China (No: 2017YFA0104400) and Jilin Province Health Science and Technology Capacity Improvement Project (No: 2021JC006).

## Conflict of Interest

The authors declare no conflict of interest.

## Supplementary Material

Supplementary material associated with this article can be found, in the online version, at <https://doi.org/10.31083/j.fbl2808186>.

## References

- [1] Fuchs Y, Steller H. Programmed cell death in animal development and disease. *Cell*. 2011; 147: 742–758.
- [2] Galluzzi L, Pedro BS, Vitale I, Aaronson SA, Abrams JM, Adam D, *et al.* Kroemer, Essential versus accessory aspects of cell death: recommendations of the NCCD 2015. *Cell Death and Differentiation*. 2015; 22: 58–73.
- [3] Thompson CB. Apoptosis in the pathogenesis and treatment of disease. *Science*. 1995; 267: 1456–1462.
- [4] Xia Y, Yuan M, Li S, Thuan UT, Nguyen TT, Kang TW, *et al.* Apigenin Suppresses the IL-1 $\beta$ -Induced Expression of the Urokinase-Type Plasminogen Activator Receptor by Inhibiting MAPK-Mediated AP-1 and NF- $\kappa$ B Signaling in Human Bladder Cancer T24 Cells. *Journal of Agricultural and Food Chemistry*. 2018; 66: 7663–7673.
- [5] Yang WS, SriRamaratnam R, Welsch ME, Shimada K, Skouta R, Viswanathan VS, *et al.* Regulation of ferroptotic cancer cell death by GPX4. *Cell*. 2014; 156: 317–331.
- [6] Dixon SJ, Lemberg KM, Lamprecht MR, Skouta R, Zaitsev EM, Gleason CE, *et al.* Ferroptosis: an iron-dependent form of non-apoptotic cell death. *Cell*. 2012; 149: 1060–1072.
- [7] Galluzzi L, Vitale I, Aaronson SA, Abrams JM, Adam D, Agostinis P, *et al.* Kroemer, Molecular mechanisms of cell death: recommendations of the Nomenclature Committee on Cell Death 2018. *Cell Death and Differentiation*. 2018; 25: 486–541.
- [8] An P, Gao Z, Sun K, Gu D, Wu H, You C, *et al.* Photothermal-Enhanced Inactivation of Glutathione Peroxidase for Ferroptosis Sensitized by an Autophagy Promotor. *ACS Applied Materials & Interfaces*. 2019; 11: 42988–42997.
- [9] Zorov DB, Juhaszova M, Sollott SJ. Mitochondrial reactive oxygen species (ROS) and ROS-induced ROS release. *Physiological Reviews*. 2014; 94: 909–950.
- [10] Moloney JN, Cotter TG. ROS signalling in the biology of cancer. *Seminars in Cell & Developmental Biology*. 2018; 80: 50–64.
- [11] Hassannia B, Vandenabeele P, Vanden Berghe T. Targeting Ferroptosis to Iron Out Cancer. *Cancer Cell*. 2019; 35: 830–849.
- [12] Li H, Wang J, Wu C, Wang L, Chen Z, Cui W. The combination of disulfiram and copper for cancer treatment. *Drug Discovery Today*. 2020; 25: 1099–1108.
- [13] Li Y, Chen F, Chen J, Chan S, He Y, Liu W, *et al.* Disulfiram/Copper Induces Antitumor Activity against Both Nasopharyngeal Cancer Cells and Cancer-Associated Fibroblasts through ROS/MAPK and Ferroptosis Pathways. *Cancers*. 2020; 12: 138.
- [14] Ren X, Li Y, Zhou Y, Hu W, Yang C, Jing Q, *et al.* Overcoming the compensatory elevation of NRF2 renders hepatocellular carcinoma cells more vulnerable to disulfiram/copper-induced ferroptosis. *Redox Biology*. 2021; 46: 102122.
- [15] McMahon A, Chen W, Li F. Old wine in new bottles: Advanced drug delivery systems for disulfiram-based cancer therapy. *Journal of Controlled Release*. 2020; 319: 352–359.
- [16] Chen Y, Yi X, Huo B, He Y, Guo X, Zhang Z, *et al.* BRD4770 functions as a novel ferroptosis inhibitor to protect against aortic dissection. *Pharmacological Research*. 2022; 177: 106122.
- [17] Stockwell BR. Ferroptosis turns 10: Emerging mechanisms, physiological functions, and therapeutic applications. *Cell*. 2022; 185: 2401–2421.
- [18] Armstrong JS. Mitochondria: a target for cancer therapy. *British Journal of Pharmacology*. 2006; 147: 239–248.
- [19] Goldman MJ, Craft B, Hastie M, Repečka K, McDade F, Kamath A, *et al.* Visualizing and interpreting cancer genomics data via the Xena platform. *Nature Biotechnology*. 2020; 38: 675–678.
- [20] Kassambara A, Kosinski M, Biecek P. survminer: Drawing Survival Curves using ‘ggplot2’. R package version 0.4.9. 2021. Available at: <https://CRAN.R-project.org/package=survminer> (Accessed: 9 March 2021).
- [21] R Core Team. R: A language and environment for statistical computing. R Foundation for Statistical Computing, Vienna, Austria. 2022. Available at: <https://www.R-project.org/> (Accessed: 31 October 2022).
- [22] Therneau T. A Package for Survival Analysis in R. R package version 3.4-0. 2022. Available at: <https://CRAN.R-project.org/package=survival> (Accessed: 9 August 2022).
- [23] Chu M, An X, Zhang D, Li Q, Dai X, Yu H, *et al.* Combination of the 6-thioguanine and disulfiram/Cu synergistically inhibits proliferation of triple-negative breast cancer cells by enhancing DNA damage and disrupting DNA damage checkpoint. *Biochimica et Biophysica Acta-Molecular Cell Research*. 2022; 1869: 119169.
- [24] Rui T, Li Q, Song S, Gao Y, Luo C. Ferroptosis-relevant mechanisms and biomarkers for therapeutic interventions in traumatic brain injury. *Histology and Histopathology*. 2020; 35: 1105–1113.
- [25] Dercho RA, Nakatsu K, Wong RJ, Stevenson DK, Vreman HJ. Determination of in vivo carbon monoxide production in laboratory animals via exhaled air. *Journal of Pharmacological and Toxicological Methods*. 2006; 54: 288–295.
- [26] Hernández-Gallardo AK, Missirlis F. Loss of ferritin in developing wing cells: Apoptosis and ferroptosis coincide. *PLoS Genetics*. 2020; 16: e1008503.
- [27] Zha J, Chen F, Dong H, Shi P, Yao Y, Zhang Y, *et al.* Disulfiram targeting lymphoid malignant cell lines via ROS-JNK activation as well as Nrf2 and NF- $\kappa$ B pathway inhibition. *Journal of Translational Medicine*. 2014; 12: 163.
- [28] Xu Y, Zhou Q, Feng X, Dai Y, Jiang Y, Jiang W, *et al.* Disulfiram/copper markedly induced myeloma cell apoptosis through activation of JNK and intrinsic and extrinsic apoptosis pathways. *Biomedicine and Pharmacotherapy*. 2020; 126: 110048.
- [29] Majera D, Skrott Z, Chroma K, Merchut-Maya JM, Mistrik M, Bartek J. Targeting the NPL4 Adaptor of p97/VCP Segregase by Disulfiram as an Emerging Cancer Vulnerability Evokes Replication Stress and DNA Damage while Silencing the ATR Pathway. *Cells*. 2020; 9: 469.
- [30] Ferreira CA, Ni D, Rosenkrans ZT, Cai W. Scavenging of reactive oxygen and nitrogen species with nanomaterials. *Nano Research*. 2018; 11: 4955–4984.
- [31] Trachootham D, Alexandre J, Huang P. Targeting cancer cells by ROS-mediated mechanisms: a radical therapeutic approach? *Nature Reviews Drug Discovery*. 2009; 8: 579–591.
- [32] Martin KR, Barrett JC. Reactive oxygen species as double-edged swords in cellular processes: low-dose cell signaling versus high-dose toxicity. *Human & Experimental Toxicology*. 2002; 21: 71–75.
- [33] NavaneethaKrishnan S, Rosales JL, Lee KY. ROS-Mediated Cancer Cell Killing through Dietary Phytochemicals. *Oxidative Medicine and Cellular Longevity*. 2019; 2019: 9051542.